# EXPERIMENTAL INVESTIGATION, MATHEMATICAL AND NUMERICAL SIMULATION OF AIRCRAFT ICING PHENOMENA

**Amelyushkin I.A.[1,2,3], Stasenko A.L.[1,2], Zhbanov V.A.[1]**
**[1]Central Aerohydrodynamic Institute*, [2]Moscow Institute of Physics and Technology*, [3]Moscow State University*, (*Russia)**

*Keywords*: **aircraft icing, supercooled droplets, ice crystals, physical mechanism of aerosol flow interaction with a solid body**

## Abstract

*Results of experimental investigation of aircraft icing physical peculiarities as well as corresponding mathematical and numerical simulation algorithms are presented. Values of energy barriers are measured for supercooled water and the corresponding temperature dependencies are presented. Models of nonspherical ice crystals' motion are developed, illustrations of numerical investigation are presented. Original approaches for molecular dynamics simulation are developed to simulate physical mechanism of aircraft icing upon structured surface.*

## Introduction

The physical foundations of multy-phase flows are common for many fields of science and industries – aerospace, energy, medical, and others. Disperse flows belong to a vast class of irreversible nonequilibrium phenomena. As a result of the interaction between the different phases, such flows are rather complicated and very difficult to be described theoretically and require special experimental methods and equipment.

Aircraft safety and ice accretion simulation are important problems in aeronautical sciences[1–4]. A multitude of investigations (both theoretical and experimental) has been devoted to these phenomena almost from the very beginning of aviation history (e.g. [2]), but the problem of anti- and deicing is far from its final solution due to the complex interrelations between the abovementioned physical processes [5–8]. The paper presented tends to reveal some their intrinsic features.

In previous publications, original algorithms were proposed to determine two-phase flow parameters in wind tunnels via laser sheet images analysis, optical system for aerosol flow with ice crystals and supercooled droplets was developed as well as the corresponding methods of flow visualization and image processing [5]. Peculiarities of supercooled droplets and nonspherical ice crystals interaction with a solid body were investigated via molecular dynamics technique [9].

## 1 Peculiarities of supercooled water crystallization

An investigation of the stability of the metastable state of a liquid and the features of its crystallization are of great interest in the modeling of aircraft icing [5, 6]. The dependences of the energy barrier necessary for the onset of crystallization of supercooled water, as well as the volume fraction of ice formed after the ice crystallization front, are obtained in [5, 6, 10]. The results can be used for aircraft icing simulation.

In present work, the effect of accumulating the kinetic energy of the impact of a supercooled liquid on a solid surface, which is necessary for crystallization, is accumulated experimentally in the form of a statistical diagram (Fig. 1 and 2).

An explanation of the effect associated with the existence of several "steps" in the investigated threshold of potential energy of intermolecular interaction is proposed. A three-dimensional diagram is constructed (Fig. 2) showing the

probability of crystallization of a metastable liquid as a function of the intensity and quantity of mechanical influences. The data obtained can be used [1,3,4] to determine the rate of ice growth and the mass flow rate of a liquid film formed by the movement of supercooled water over the surface of a streamlined body in order to predict the modes of aircraft icing. New results of thermal imaging and measurement of parameters characterizing the features of crystallization of a metastable liquid are presented in [6].

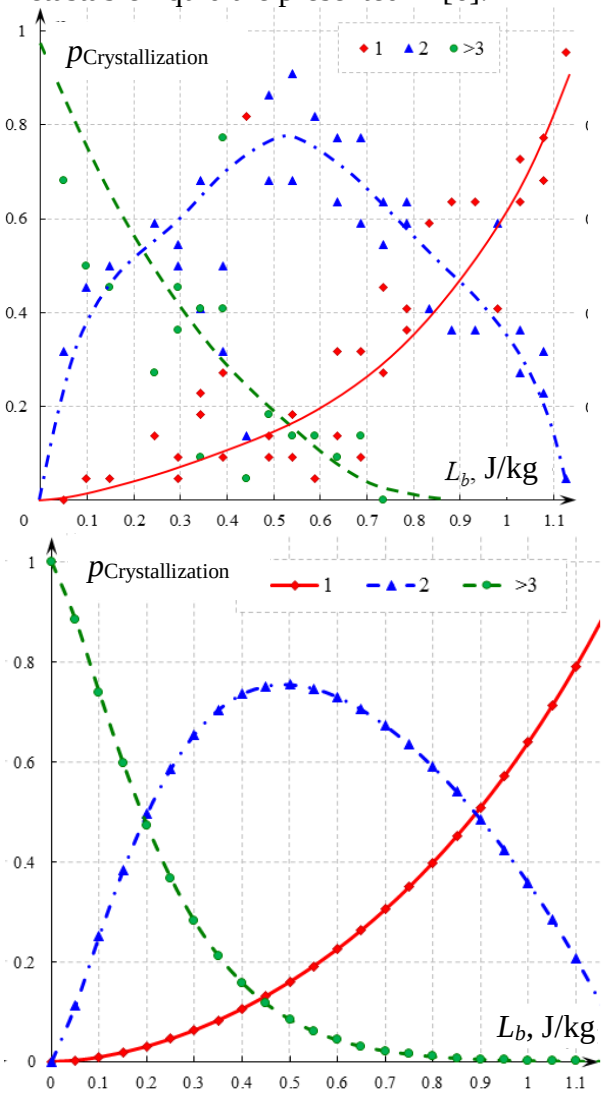


Fig. 1: The probability of crystallization $p$ as a function of the intensity and quantity (1, 2, 3 or more) of mechanical influences; $L_b$ – the height of the potential barrier of a metastable liquid, $L_b^0 = 4$ mJ/kg. Above – initial experimental data, beneath – corresponding numerical approximation.

Dozen of years ago a similarity of processes was noted [11], which are being accompanied by the overcoming of a barrier between two states of matter, for example, in chemical reactions, thermonuclear transformations [12], electrical and optical discharges, solid solutions, crystallization of metastable liquid [13], sintering of metal powders. The moving interface of phases or reacting components has specific properties [5, 6, 10, 13, 14].

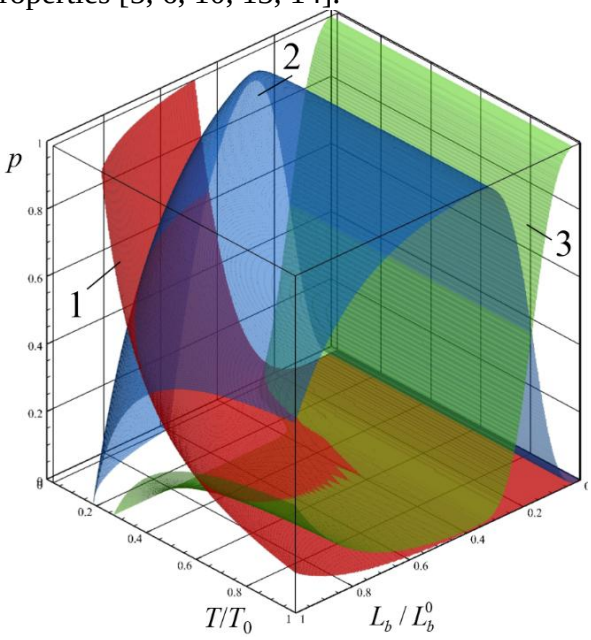


Fig. 2: Three-dimensional statistical diagram of the stability of supercooled water subjected to mechanical influences.

A general expression is proposed for describing the propagation of the rate of crystallization and the detonation wave) by the relation:

$$u^2 = \chi\left(\frac{T}{T_f}\right)^m Z \exp\left(-\frac{L_b}{RT}\right)\left(\frac{T_f - T}{T_f}\right)^{m+1},$$

Here $T$ – initial temperatue, $\chi = \lambda/\rho C_p$ temperature conductivity of matter before the front ($\lambda$ – thermal conductivity coefficient, $\rho$ – density, $C_p$ – specific heat capacity), index $b$ means "barrier" in phase transition. The characteristic temperature is the value of the phase transition temperature (for water $T_f$=273 K). The second, third, and fourth factors in the expression correspond to the Arrhenius formula; the value of $Z$ is of dimension $s$–1, and $R$ is the specific gas constant. The last factor takes into account that for $T = T_f$ one has $u = 0$, the exponent m in the case of a chemical reaction represents its order. In the case of supercooled water, complex quantum-mechanical studies would be required to determine $m$, the barrier

height $L_b$, and the pre-exponential factor $Z$. In this paper estimates of these quantities are made on the basis of experimental studies. In comparison with [6] one has $m$=3.

## 2 Non-spherical ice crystals' motion simulation

The modeling of nonstationary motion of nonspherical bodies in inhomogeneous flows, as well as the dynamics of heterogeneous flows containing crystals of complex shape is of great practical interest in a wide range of engineering fields, phenomena of nature and human life [6,8]. In the study and formation of models of the dynamics of dispersed flows and the development of appropriate computer simulation algorithms, the assumption is generally made of the spherical particles and the droplets of the dispersed phase in the heterogeneous flow. This assumption is fully justified in various practical applications, but in many technological and natural processes, spherical forms can lead to serious errors. In [6, 8], a significant influence of the ratio of longitudinal and transverse semi-axes of spheroids on the distribution along the surface of the streamlined body of the mass flow of the dispersed phase and the region of inertial precipitation of the disperse phase on the surface of the aircraft during the icing process is shown.

The mechanics of a nonequilibrium multiphase medium naturally begins with the dynamics of an individual spherical particle (see, for example, [15, 16]). In this case, even for the sphere there are many mathematical expressions, various semi-empirical data on the drag coefficient $C_D(\boldsymbol{V}-\boldsymbol{V_p}, \mathrm{M}_p, \mathrm{Re}_p, \ldots)$, e.g., [17]. The exceptions are special cases of creeping motion (Stokes force) and free-molecular mode of the carrier medium ($\mathrm{Kn}_p = l_m/2a_p >> 1$), for which "exact" formulas exist. Drag force $F_D$ is assumed to be applied to the center of the ball particle.

Thus, the dynamics of a nonspherical particle must be described by integro-differential equations. For the case of acicular crystals this problem was begun in [5–7].

The complex problem of the dynamics of an individual particle or a drop that collides with a solid is studied by the molecular dynamics method.

Due to the immense variety of particle shapes (in particular, ice crystals), it is highly desirable to develop a criterion for optimal detailing the study of their dynamics. In particular, flattened and elongated ellipsoids are recognized as fairly representative, the limiting forms of which are the rod, the ball, and the disk.

To characterize the degree of difference in the shape of a nonspherical particle from a sphere, the so-called "sphericity" $\Phi$ is the ratio of the surface area of a non-spherical particle to the surface area $4\pi a_p^2$ of the volume-equivalent sphere[18].

The force that acts on a particle may be taken as follows [6, 8]:

$$< \boldsymbol{F}(\mathrm{Re},\mathrm{M}) >= \boldsymbol{F}_\mathrm{A} = \frac{\iiint \boldsymbol{F}(\mathrm{Re},\mathrm{M},\varphi,\theta,\psi)\,\mathrm{d}\varphi\mathrm{d}\theta\mathrm{d}\psi}{\iiint \mathrm{d}\varphi\mathrm{d}\theta\mathrm{d}\psi}$$

Integrals are taken over all orientations of a particle. The expression for the mean square deviation (i.e. orientational force) is:

$$F_\chi = \sqrt{\frac{\iiint \left(\boldsymbol{F}(\mathrm{Re},\mathrm{M},\varphi,\theta,\psi) - \boldsymbol{F}_\mathrm{A}\right)^2 \mathrm{d}\varphi\mathrm{d}\theta\mathrm{d}\psi}{\iiint \mathrm{d}\varphi\mathrm{d}\theta\mathrm{d}\psi}}$$

The expression for the scattering coefficient of nonspherical particles has the following form: $S_\chi = \sqrt{F_\chi / \rho_p}$ ; $\rho_p$ – density of particles' material. In contrast to the temperature of a molecular gas, the temperature of a "gas" (χαος) of nonspherical particles is estimated from their heat capacity and the speed of randomized motion.

Numerical algorithm for calculating trajectories' stochastics of randomized particles: At each step in time, the stochastic acceleration of the particle $\boldsymbol{\Xi}\sqrt{2S}\cdot\xi$ is added. Here $\xi$ – random number, uniformly distributed from 0 to 1, $\boldsymbol{\Xi}$ – random unit vector, $S$ – scattering coefficient. Thus, the equation for the stochastic motion of a particle will have the following form:

$$m_p \frac{\mathrm{d}\boldsymbol{V_p}}{\mathrm{d}t} = \sum \boldsymbol{F}_{\mathbf{Det}} + m_p \sum_{k=1}^{k_{\max}} \boldsymbol{\Xi}_k \sqrt{2S_k}\cdot\xi_k$$

The sum is taken over all $k$ possible mechanisms of stochastic particle movements, $m_p$ – mass of a

particle. Some of them are: turbulent flow pulsations; nonspherical form of particles; brownian motion of small particles and surrounding molecules; chaotization particles' collisions with each other as well as with a circumfluent body.

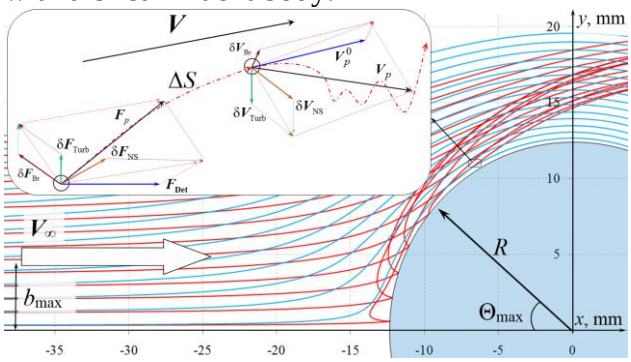


Fig. 3: Scheme for calculating stochastic particle dynamics.

For each type of physical mechanism of stochastics, the diffusion coefficients are calculated and inserted into the last formula.

In present paper, we consider stochastics, which is based on nonspherical shape of particles.

Now then, the orientation force $F_\chi$ which acts on a particle could be described by the following equation ($Re_p$<<1):

$$\boldsymbol{F}_\chi(\mathrm{Re}) = 3\pi\frac{\mu^2}{\rho}\mathrm{Re}_p\left|1-\frac{1}{E^{1/3}}\sqrt{\frac{E^2+4E+5}{10}}\right|$$

Stabilization coefficient is defined from dimension analysis:

$$S_\chi \sim V_\chi L_\chi; \qquad F_\chi A_\chi = F_\chi\frac{S_\chi}{V_\chi} \sim \frac{m_p V_\chi^2}{2}$$

So one can obtain the expression for stabilization coefficient:

$$\Gamma_\chi \sim \frac{F_\chi}{V_\chi} = F_\chi\left(\frac{m_p}{F_\chi S_\chi}\right)^{1/3} = F_\chi\left(\frac{m_p}{F_\chi\sqrt{F_\chi/\rho_p}}\right)^{1/3}$$

As a result the equation for nonspherical particles' stochastic and deterministic motion will be as follows:

$$m_p\frac{\mathrm{d}\boldsymbol{V_p}}{\mathrm{d}t} = \sum\boldsymbol{F}_{\mathbf{Det}} - \Gamma_\chi\boldsymbol{V_p} + \delta(t)\Xi_{\mathrm{NS}}F_\chi\cdot\xi_\chi$$

In spite of a lot of different mathematical models for aerohydrodynamic characteristics of single nonspherical particles, simulation [10, 11, 13] of the whole two-phase flow with nonspherical particles becomes problematic.

Let us write down the equation for the change in the chaotic energy of nonspherical particles under the assumption that there are no phase transitions and temperature nonequilibrium:

$$\frac{\mathrm{d}}{\mathrm{d}t}\frac{m_p V_\chi^2}{2} = F_\chi\left|\boldsymbol{V}-\boldsymbol{V}_p\right|$$

$$\frac{\mathrm{d}W_\chi}{\mathrm{d}t} = \frac{\partial W_\chi}{\partial t} + \left(\boldsymbol{V}-\boldsymbol{V}_p\right)\overline{\nabla}W_\chi = \frac{F_\chi\cdot V_\chi}{m_p} - \Gamma_\chi V_\chi\left|\boldsymbol{V}-\boldsymbol{V}_p\right|$$

In the last equation, the first term describes the production of chaotic energy, the second one describes the dissipation of this energy; here

$$F_\chi = \left|1-\sqrt{\frac{f_\parallel^2+f_\perp^2}{2}}\right|6\pi a\mu\left|\boldsymbol{V}-\boldsymbol{V}_p\right| =$$

$$= 6\pi a\mu\left|\boldsymbol{V}-\boldsymbol{V}_p\right|\varphi = 3\pi\frac{\mu^2}{\rho}\mathrm{Re}_p\,\varphi,$$

$$\varphi = \left|1-\sqrt{\frac{f_\parallel^2+f_\perp^2}{2}}\right| \approx \left|1-\frac{1}{E^{1/3}}\sqrt{\frac{E^2+4E+5}{10}}\right|.$$

Being based on the values of the scattering force, the scattering coefficient and the mass particle determining the inertia, one has:

$$V_\chi = \left(\frac{F_\chi S_\chi}{m_p}\right)^{1/3} = \frac{\mathrm{Re}_\infty LV_\infty}{a_p}\sqrt{3\pi\frac{\rho}{\rho_p}\mathrm{Re}_p\,\varphi}\left(\frac{3}{4\pi}\right)^{1/3}$$

So, the dependence of the velocity of the chaotic motion of the particle as a function of the Reynolds number $\mathrm{Re_p}$ of its motion relative to the gas, the ratio of the gas densities, the particle and the ratio of the characteristic dimensions of the streamlined body and the volume-equivalent spherical particle is as follows:

$$\frac{V_\chi}{V_\infty} = \mathrm{Re}_\infty\frac{L}{a_p}\sqrt{\frac{\rho}{\rho_p}}\sqrt{\mathrm{Re}_p\,\varphi}\left(\frac{243}{16}\pi\right)^{1/6}$$

The characteristic frequency of pulsations is obtained from the following expression:

$$\omega_\chi = \frac{F_\chi}{m_p}\left(\frac{m_p}{F_\chi S_\chi}\right)^{1/3} = \mathrm{Re}_\infty\frac{L}{a_p}\frac{V_\infty}{a_p}\sqrt{\frac{\rho}{\rho_p}}\sqrt{\mathrm{Re}_p\,\varphi}\frac{3}{2}\left(\frac{3}{4\pi}\right)^{1/6}$$

Thus, the dimensionless particle pulsation frequency in an inhomogeneous flow has the following form:

$$\frac{\omega_\chi a_p}{V_\infty} = \mathrm{Re}_\infty\frac{L}{a_p}\sqrt{\frac{\rho}{\rho_p}}\sqrt{\mathrm{Re}_p\,\varphi}\frac{3}{2}\left(\frac{3}{4\pi}\right)^{1/6}.$$

**Table: Parameters of gas (chaos) of nonspherical particles in dimensionless form**

| | |
|---|---|
| Orientation force | $F_\chi / F_{\text{Stk}} = \varphi$ |
| Scattering coefficient | $\frac{S_\chi}{\mu/\rho} = \frac{\rho}{\mu}\sqrt{\frac{F_\chi}{\rho_p}} = \sqrt{\frac{\rho}{\rho_p}}\sqrt{3\pi \operatorname{Re}_p \varphi}$ |
| Velocity | $\frac{V_\chi}{V_\infty} = \operatorname{Re}_\infty \frac{L}{a_p}\sqrt{\frac{\rho}{\rho_p}}\sqrt{\operatorname{Re}_p \varphi\left(\frac{243}{16}\pi\right)}^{1/6} \cong 1.9 \operatorname{Re}_\infty \frac{L}{a_p}\sqrt{\frac{\rho}{\rho_p}}\sqrt{\operatorname{Re}_p \varphi}$ |
| Length | $\frac{A_\chi}{a_p} = \frac{1}{3}\sqrt{\frac{\rho_p}{\rho}}\sqrt{\frac{\operatorname{Re}_p}{\varphi}}\frac{(4\pi/3)^{1/6}}{\operatorname{Re}_\infty^2}$ |
| Frequency | $\frac{\omega_\chi a_p}{V_\infty} = \operatorname{Re}_\infty \frac{L}{a_p}\sqrt{\frac{\rho}{\rho_p}}\sqrt{\operatorname{Re}_p \varphi}\frac{3}{2}\left(\frac{3}{4\pi}\right)^{1/6} \cong 1.2 \operatorname{Re}_\infty \frac{L}{a_p}\sqrt{\frac{\rho}{\rho_p}}\sqrt{\operatorname{Re}_p \varphi}$ |
| Stabilization coefficient | $\frac{\Gamma_\chi}{\rho V_\infty \pi a_p^2/2} = 12\frac{L}{a_p}\frac{\varphi}{\operatorname{Re}_\infty}$ |
| Pressure | $\frac{P_\chi}{\rho V_\infty^2} = \frac{\rho_p^V}{\rho_p}\left(\frac{\operatorname{Re}_\infty L}{a_p}\right)^2 \operatorname{Re}_p \varphi\left(\frac{243}{16}\pi\right)^{1/3}$ |

Than characteristic amplitude of pulsations can be estimated from the following expression:

or $A_\chi \cong \frac{|\boldsymbol{V}-\boldsymbol{V}_p|}{\omega_\chi} = \sqrt{\frac{\rho_p}{\rho}}\sqrt{\frac{\operatorname{Re}_p}{\varphi}}\frac{a_p}{\operatorname{Re}_\infty^2 3}\left(\frac{4\pi}{3}\right)^{1/6}$

Table illustrates the calculated parameters of the gas (chaos) of nonspherical ice particles in inhomogeneous flows in a dimensionless form.

In the stationary flow, integrating along the deterministic trajectories of the particles, one can rewrite the equation of energy transfer of chaos in the following form:

$$(\boldsymbol{V}-\boldsymbol{V}_p)\frac{1}{2}\frac{dV_\chi^2}{ds} = \frac{F_\chi \cdot V_\chi}{m_p} - \Gamma_\chi V_\chi |\boldsymbol{V}-\boldsymbol{V}_p| \qquad \text{or:}$$

$$\frac{2}{9}\frac{\rho_p a_p^2}{\mu\varphi}\frac{dV_\chi}{ds} = 1 - \frac{1}{3}\left(\frac{3}{4\pi}\right)^{1/6}\sqrt{\frac{\rho_p}{\rho}\operatorname{Re}_p \varphi}$$

Expressing the first term in terms of the Stokes number $\text{Stk} = \frac{2\rho_p V_\infty}{9\mu L}a_p^2 = \frac{2\rho_p a_p^2}{9\mu}\frac{V_\infty}{L}$, one has: $\frac{\text{Stk}}{\varphi}\frac{L}{V_\infty}\frac{dV_\chi}{ds} = 1 - \frac{1}{3}\left(\frac{3}{4\pi}\right)^{1/6}\sqrt{\frac{\rho_p}{\rho}\frac{\operatorname{Re}_p}{\varphi}}$

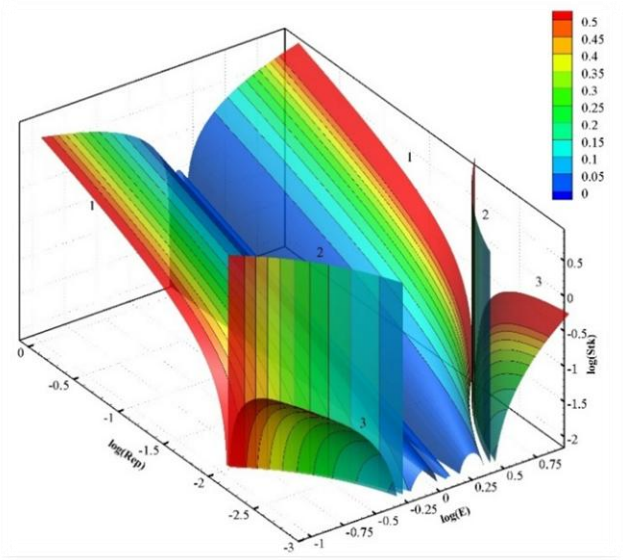


Fig. 4: Dependence of the chaotization coefficient on the parameters of gas flow around a particle: 1 – $a_\chi$ = –1; 2 – $a_\chi$ = 0; 3 – $a_\chi$ = 1.

According to this model, the motion of a non-spherical particle is stable when $\frac{\rho_p}{\rho}\frac{\operatorname{Re}_p}{\varphi} > 3\sqrt[3]{36\pi} \cong 14.51$.

A parameter that characterizes the increase in the velocity of chaotic motion of particles (referred to the characteristic flow velocity $V_\infty$) has the following form:

$$\frac{dV_\chi}{ds} = a_\chi = \frac{\varphi}{\text{Stk}}\left(1 - \frac{1}{3}\left(\frac{3}{4\pi}\right)^{1/6}\sqrt{\frac{\rho_p}{\rho}\frac{\operatorname{Re}_p}{\varphi}}\right).$$

## 3 Molecular physics simulation of aerosol flow interaction with a solid body

Simulation of boundary conditions as well as surface flow control is essential in various areas of industry, science, technology, e.g. aircraft icing simulation. Processes of atmospheric gas molecules diffusion as well as crystalline grains are described in classical monographs which are devoted to icing physics (e.g., [6]). However, specifics of problems under investigations concludes necessity of description of hydro-thermodynamics of mass transfer of air-droplets'-crystalline flow with non-ideal smooth surface of a solid body in a shear flow of carrying gas where microturbulent pulsations happen due to roughness of a circumfluent surface.

The main tasks of the elaborated program are: prediction and optimization of the flow interaction with the streamlined body, calculation of the collision regimes of particles and droplets with a solid surface, calculation of the circumfluent characteristics of bodies by the flow of liquid, gas and plasma modeling the boundary conditions on the surface, investigation and control of flow turbulence, wetting modeling and the motion of drops on surfaces. In this paper, we present the results of calculating the characteristics of a three-dimensional unsteady boundary layer of a multicomponent real gas near a streamlined body of various materials with different roughnesses.

As a rule, the icing investigations carried out recently are based on experimental data and phenomenological description of the icing process. However, for the successful problem solution it is necessary to develop mathematical models which take into account physical processes accompanying ice accretion on fundamental level.

But real walls are always rough. In particular, the experiments have shown [20] that the flow even in a viscous sublayer is accompanied by appreciable turbulent pulsations. One also notes the following circumstance: aerodynamic techniques are characterized by surfaces with an average roughness of the order of $h \sim 1$ μm. With increasing altitude of flight, the mean free path $l_m$ of air molecules approaches this value. Therefore, the continual description of the generation of turbulence on the micro-roughness of the surface must be revised on the basis of the molecular dynamics method which allows one to take into account the influence of the Knudsen number. According to this investigation, the short-wavelength (atomistic) roughness is not very important. For rough hydrophobic surfaces, there is no contact angle hysteresis $\theta_A - \theta_R$ (indices A, R – advancing and receding surface tension angles) due to strong thermal fluctuations, which occur at the liquid-solid interface on the nanoscale (Fig. 5). Similar investigations were carried out in [21]; however, in this paper there is no information about validity of the presented results which should be compared with those obtained by other investigators. An experimental investigation of droplets' evaporation on hydrofilic surfaces was carried out in [22].

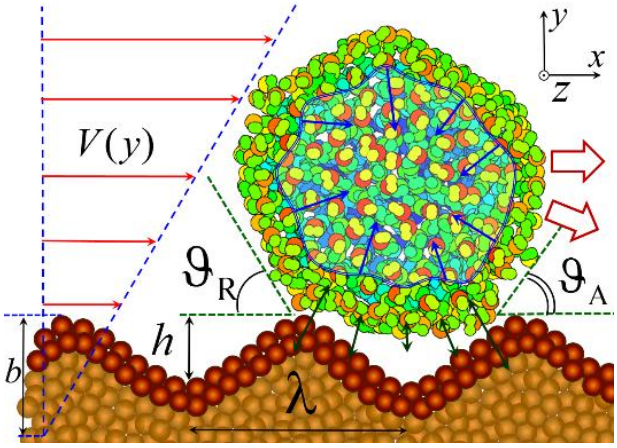


Fig. 5: Scheme for controlling the interaction of the flow with a nanorelief of a solid body having different degrees of hydrophobicity.

In the plane $x = 0$, the mass flow $q = \rho V$ was set. As the plane $x = L$ and $y = H$ are passed, the molecules leave the computational domain (Fig. 5). In this case, in the planes $x = 0$, $x = L$ and $y = H$, an additional mass flow is specified, which is due to the thermal motion of the molecules: $q_x = q_y = \rho < V > / 2\sqrt{3} = \rho\sqrt{RT} / 2$. In the lower part of the calculated region, there was a rough surface of the streamlined body, the interaction with which was subordinated to the mathematical models defined below. At the "bottom" of the cubic region, water and air molecules interact with solid-state atoms, depending on their physical properties and wall temperature. Correspondent conditions are described in [9].

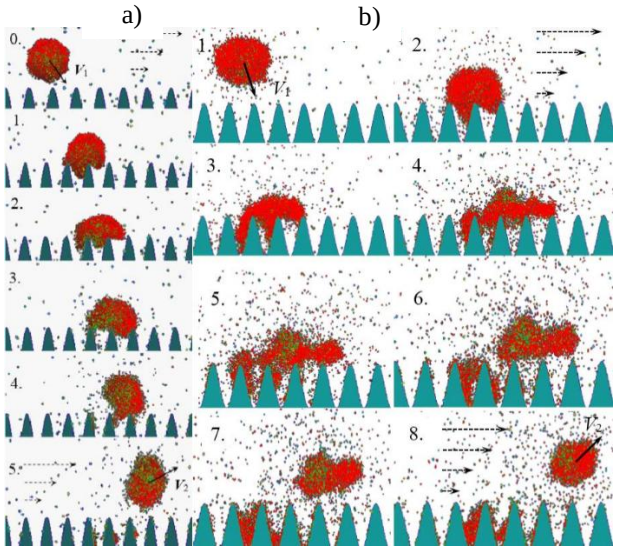


Fig 6: Calculations of droplets' interaction with circumfluent surfaces via molecular dynamics technique: a) – initial number of water molecules $N$ = 2500, impingement velocity is 100 m/s, normal conditions, $h = 8\sigma_0$; b) results of calculations for the same parameters as in a center, but $N$ = 4600.

The characteristic height $h$ and length $\lambda$ of periodic roughness are chosen as the main control parameters, and the parameter $AK = \varepsilon_{w\text{-}m} / \varepsilon_{m\text{-}m} \approx 0.5\ (1 + \cos\theta)$, which can be treated as the ratio of the energies $\varepsilon_{w\text{-}m}$ of the interaction between the flux molecule and the atom surface (adhesion) to the characteristic energy $\varepsilon_{m\text{-}m}$ of the interaction of the flow molecules with each other (cohesion), and $\theta$ is the wetting angle.

In Fig. 6 one can see examples of droplets' impingement on rough surfaces in a shear gas flow; $\sigma_0 \approx 0.26$ nm– characteristic length of intermolecular interaction. Parameters of the interaction of molecules are derived on the basis of the characteristics of the real gas equation of state and taken from the reference data concerned parameters of intermolecular interaction, and also from quantum chemical calculations of the interaction energy of the flow molecules with different atoms of the circumfluent body.

One can easily see the fragmentation of the droplet and its tight attachment to impurities of the rough surfaces for larger velocities value and rebound for the less one.

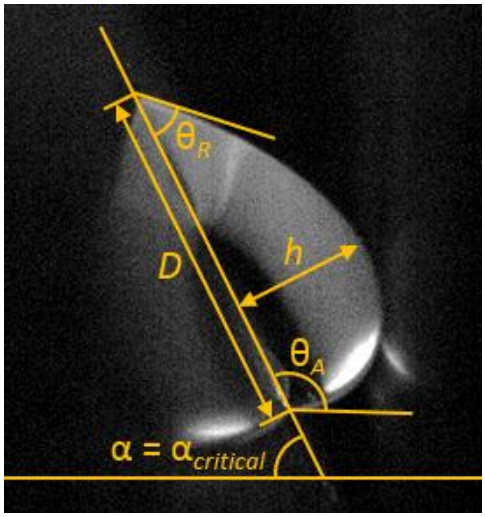


Fig 7: Photo of droplet on inclined surface: $\theta_A$ – advancing angle, $\theta_R$ – receding angle, $\alpha$ – angle of inclined surface, $D$ – diameter of contact spot, $h$ – height of the droplet.

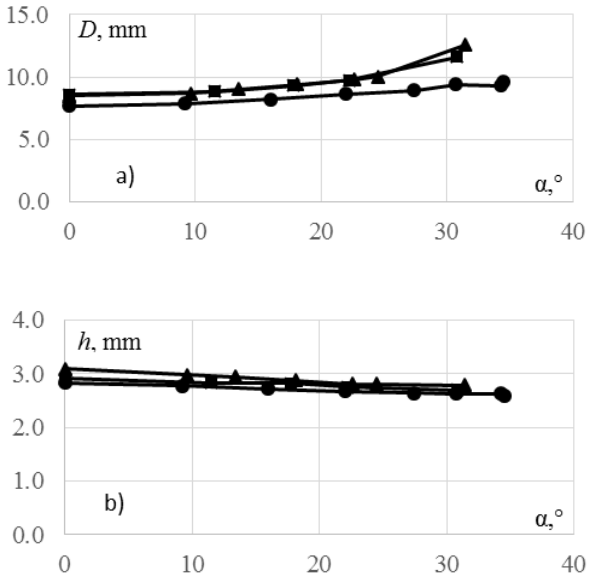


Fig 8: Dependences of droplet contact spot diameter a) and droplet height (b) as a function of inclined surface angle.

## 4. Large droplets' motion investigation

As the first step to understanding of large droplet movement upon a solid surface, critical values of $\theta_A$ and $\theta_R$ are measured in the case of inclined plate, when the gravity force simulates the aerodynamic one. Droplets parameters, such as height $h$ and contact spot diameter, static, advancing and receding angles were experimentally measured for more accurate process simulation [23]. Fig. 8 and 9 show experimental dependencies of droplet's parameter on angle of inclined surface (Fig. 7).

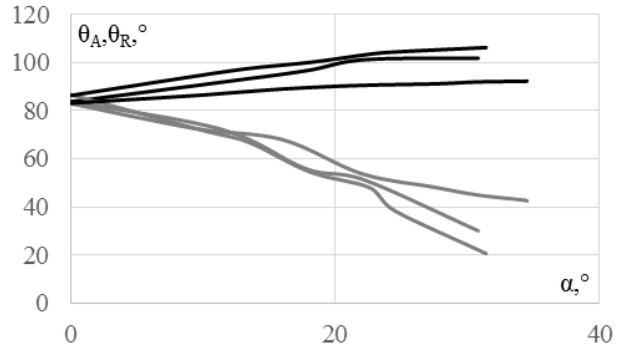


Fig 9: The dependence of droplet advancing angle (black curves) and receding angles (grey curves) as a function of inclined surface angle.

## Conclusion

Results of supercooled water crystallization peculiarities investigation are presented. Original models for nonspherical ice crystals in non-uniform flows are presented. Mathematical models, numerical algorithms and programs for calculating the interaction of gas and disperse systems with a nanostructured surface of solids of various materials have been developed, which allow modeling boundary conditions on a streamlined surface controlling the flow interaction with the body, calculating the collision regimes of particles and droplets with a solid, flow characteristics, investigating microvortical and turbulent flows, and simulating wetting and droplet movement over the surface. Taking into account the peculiarities of molecular effects in a thin layer near the relief body, the developed program allows to reconsider the mechanism of aircraft icing on the surface roughness. The developed methodology allows us to specify physical mechanism of flow interaction with a solid body, as well as a single droplet or ice crystal with nanostructured relief of the circumfluent body surface.

## Acknowledgement

These investigations were supported by grant of Russian scientific foundation (**RNF**): project No 16–19–10472 (**parts 1, 3, 4**) and by Russian Fund for Basic Research (**RFBR**): project No 18-31-00485 (**part 2**).

## References

[1] Bourgault Y, Beaugendre H and Habashi WG. Development of a shallow water icing model in FENSAP-ICE. *AIAA Journal of Aircraft*, Vol. 37, pp 640-646, 2000.

[2] Bachalo WD, Sipperley C and Payne G. Aircraft icing research: challenges in cloud simulation and characterization ILASS Americas. *23-nd Annual Conference on Liquid Atomization and Spray Systems*, Ventura, CA., May 2011; Disc; paper No. 3, pp 1-14, 2011.

[3] Miller AB, Potapov YuF and Stasenko AL. Experimental and theoretical investigation of aircraft icing in the case of crystal and mixed-phase flow. *29th Congress of the International Council of the aeronautical sciences*; September 7th–12th 2014; St-Petersburg; Russia, Paper No. 0576, pp 1-6, 2014.

[4] Hallett J and Isaac GA. Aircraft icing in glaciated and mixed phase clouds. *J. Aircraft*, Vol. 45, No. 6, pp 2120-2130, 2008.

[5] Amelyushkin IA. Supercooled water crystallization in a problem of ice accretion. *Journal of Visualization of Mechanical Processes*, Vol. 4, Issue 1, pp 1-18, 2016.

[6] Amelyushkin IA and Stasenko AL. Interaction of supercooled droplets and nonspherical ice crystals with a solid body in a mixed cloud // CEAS Aeronautical Journal, pp 1–10, 2018.

[7] Amelyushkin IA and Stasenko AL. Interaction of gas flow carrying nonspherical microparticles with transversal cylinder. *J. Phys. Engineering*, Vol. 91, No. 3, pp 307-318, 2018.

[8] Amelyushkin IA. Mathematical models and optical investigation of two phase flows in wind tunnels. *Proceedings from the 30th Congress of the International Council of the Aeronautical Sciences* ICAS-2016 25th–30th September 2016; Daejeon, Korea, paper No 2016_0665, pp 1-5, 2016.

[9] Amelyushkin IA and Stasenko AL. Simulation of aerosol flow interaction with a solid body on molecular level. *AIP Journal, Conference series*, 2018. DOI: 10.1063/1.5034629.

[10] Hallet J. Experimental studies of the crystallization of supercooled water. *J. of the Atm. Sciences*, Vol. 21, pp 671-682, 1964.

[11] Merzhanov AG and Rumanov EN. Thermal processes like combustion in physics. Preprint of Institute of Chemical Physics (IChPh), USSR Academy of Science. Chernogolovka, Moscow region, Russia, 1975. (in Russian).

[12] Zeldovich YaB, Barenblatt GI, Librovich VB and Mahviladze GM. Mathematical theory of combustion and explosion. *Science*, Moscow, 1980. (in Russian).

[13] Polezhaev YuV and Stonik OG. Physical basis of combustion. *Hight Temperature*, Vol. 48, No. 6, pp 981, 2010. (in Russian).

[14] Pisarev VV. Fetermination of crystal-melt free energy. *Hight Temperature*, Vol. 50, No 6, pp 769, 2012. (in Russian).

[15] Vancenzi D. Orientation of nonspherical particles in an axisymmetrical random flow. J. *Fluid. Mech*. Cambridge Univercity Press, Vol. 719, pp 465-487, 2013.
[16] Nilamdeen S and Habashi WG. Multiphase approach toward simulating ice crystal ingestion in jet engines. *J. Propulsion and Power*, Vol. 27, No. 5, pp 959-969, 2011.
[17] Molleson GV and Stasenko AL. Interaction of a two-phase jet with a solid body with generation of a "chaos" of particles. *Hight Temperature*, Vol. 51, No. 4, pp 537-550, 2013.
[18] Höltzer A and Sommerfeld M. New simple correlation formula for the drag coefficient of nonspherical particles. *Powder Technology*, Vol. 184, No. 3, pp 361-365, 2008.
[19] Hobbs PV. Ice Physics. *Oxford Univ. Press*, Oxford, 2010.
[20] Speziale CG, Sackar S and Gatski TB. Modelling the Pressure-Strain Correlation of Turbulence: An Invariant Dynamical Systems Approach *J. Fluid Mechanics*, Vol. 227, pp 245-272, 1991.
[21] Yang C, Tartaglino U and Persson BNJ. Nanodroplets on rough hydrophilic and hydrophobic surfaces. *Eur. Phys. J.* E 25, Vol. 25, Issue 2, pp 139-152, 2008.
[22] Xuemei Chen, Ruiyuan Ma, Jintao Li, Chonglei Hao, Wei Guo, Luk BL, Shuai Cheng Li, Shuhuai Yao and Zuankai Wang. Evaporation of droplets on superhydrophobic surfaces: surface roughness and small droplet size effects. *Phys. Rev. Let.*, Vol. 109, pp 116101-1-116101-6, 2012.
[23] Stasenko AL and Zhbanov VA. Together on inclined surface. *Kvant Journal*, No. 3, pp 34-36, 2018. (in Russian).

**Contact Author Email Address**

Amelyushkin_Ivan@mail.ru
Stasenko@serpantin.ru
Zhbanov@physics.msu.ru

## Copyright Statement